Bacterial turgor pressure can be measured by atomic force microscopy

Markus Arnoldi,[1] Monika Fritz,[1] Edmund Bäuerlein,[2] Manfred Radmacher,[3] Erich Sackmann,[1] and Alexei Boulbitch[1,*]
[1]*Physik Department, Institut für Biophysik, E22, Technische Universität München, James-Franck-Strasse, 85747 Garching bei München, Germany*
[2]*Abteilung für Membranbiochemie, Max-Planck-Institut für Biochemie, Am Klopferspitz 18a, 82152 Martinsried, Germany*
[3]*Sektion Physik, Lehrstuhl für Angewandte Physik, LMU München, Amalienstrasse 54, 80799 München, Germany*
(Received 29 November 1999)

We report a study of the deformability of a bacterial wall with an atomic force microscope (AFM). A theoretical expression is derived for the force exerted by the wall on the cantilever as a function of the depths of indentation generated by the AFM tip. Evidence is provided that this reaction force is a measure for the turgor pressure of the bacterium. The method was applied to magnetotactic bacteria of the species *Magnetospirillum gryphiswaldense*. Force curves were generated on the substrate and on the bacteria while scanning laterally. With the mechanical properties so gained we obtained the spring constant of the bacterium as a whole. Making use of our theoretical results we determined the turgor pressure to be in the range of 85 to 150 kPa.

PACS number(s): 87.64.Dz, 87.17.Aa, 87.19.Rr, 87.16.Gj

I. INTRODUCTION

Bacteria can be divided into two classes: the so-called gram-negative and gram-positive bacteria, depending on their ability to be stained by the Gram technique. The envelope of gram-negative bacteria is composed of two subshells: the inner cytoplasmic membrane, serving as the major permeability barrier, and the outer membrane. The inner layer of the outer subshell consists of phospholipids and the outer of lipopolysaccharides. It also contains proteins called porines which form channels. The cell wall—consisting of peptidoglycan—lies between the outer and the inner subshells, in the so-called periplasmic space, and is linked with the outer shell via lipoproteins. The cell walls of gram-negative bacteria are thin (about 30 to 80 Å [1]). Gram-positive bacteria have only a single plasma membrane and no outer membrane or periplasmic space. Their peptidoglycan layer is thicker than that found in gram-negative organisms, being about 250 Å [1,2]. The internal volume of bacteria is filled with cytoplasm containing an actin gel which is, however, too soft to maintain the shape of the living cell. The shape is maintained by the large difference between the inner and the outer osmotic pressure (higher in the cytoplasm) which is called the turgor pressure. For gram-positive bacteria this pressure difference is about 20 to 50 atm [3,4]. For gram-negative bacteria the turgor pressure is reported in the range from 0.8 atm for cyanobacteria [5] to 3–5 atm [6–9]. The turgor pressure plays an important role in control of the behavior of bacterial cells. Changes in the turgor pressure cause stress on the membrane and induce the expression of osmoregulatory genes. Several functions of bacterial cells are regulated by the turgor pressure, including bacterial signal transduction systems, bacterial periplasmic transport functions, synthesis of porines, expression of the operon that codes for the transport system responsible for K^+ uptake in *Escherichia coli*, and synthesis of the cholera toxin in *Vibrio* [10–12]. It is therefore of paramount interest to measure the turgor pressure and to study the bacterial reactions to changes of osmolarity. A first method for the determination of the bacterial turgor pressure was proposed by Mitchell. It is based on the measurement of water uptake by predried bacterial paste [13]. Later, the bacterial turgor pressure was studied by several techniques, such as turbidity measurements by light scattering, light microscopy, and application of labeled molecules [14].

All bacteria are able to adapt themselves within certain limits to the osmotic environment. The mechanisms of adaptation are understood rather well [12], whereas characteristic response times of the osmoregulation mechanisms are still unknown. Observations made by stop-flow measurements [14] yielded estimates of characteristic response times ranging from several tens of seconds to a few minutes. Most experiments reported in the literature to determine the turgor pressure have been subjected to the criticism that the cell's response mechanisms may have caused a change in the internal osmotic pressure before the measurements could be completed (for a recent review see [14]). This problem is overcome in the method of turgor pressure measurements by collapse of gas vesicles in the cytoplasm which was pioneered by Walsby, Hayes, and Boje [5]. These are hollow cylinders composed of proteins which are filled with air and are referred to as vesicles in bacteriological literature. They are found in some families of bacteria, including halophiles, cyanobacteria, and methanogens. Other bacteria (such as *E. coli*) do not possess such vesicles. In the above mentioned method the pressure applied to the external medium that causes collapse of the vesicles is measured under natural conditions and again after the removal of the turgor pressure. The difference between the two collapse pressures yields the bacterial turgor pressure. The collapse is detected by light scattering [14]. This method is only applicable to bacteria possessing vesicles.

Recently, micromechanical techniques have been applied

*Author to whom correspondence should be addressed. FAX: 49 (89) 2891 2469. Electronic address: aboulbit@physik.tu-muenchen.de

to studying bacteria. The optical tweezers technique was applied to manipulate *E. coli* [15]. Atomic force microscopy (AFM) has also attracted growing interest in bacteriology [16–21]. Up to the present AFM has been mainly applied for qualitative characterization of bacteria. Both gram-positive and gram-negative bacteria have been studied with this technique [17,16]. Morphological studies of *E. coli* exposed to antibiotics have been reported by Braga and Ricci [18]. It was further shown that AFM can be applied to measure the force of interaction between a bacterium and a surface [19]. It has also been used to measure the Young's modulus of the dried sheath of the archaebacterium *Methanospirillum hungatei* [20,21].

In the present paper we report atomic force microscopy studies of the gram-negative bacterium *Magnetospirillum gryphiswaldense*. We present a detailed theoretical analysis of deformation of the bacterial envelope caused by the AFM cantilever. We show that measurements of the rigidity of the bacteria by the AFM technique enable the determination of the bacterial turgor pressure. In particular, we have determined the turgor pressure of *Magnetospirillum gryphiswaldense*.

The paper is organized as follows. In Sec. II we briefly present the theory of local deformations of adhering bacteria. The detailed discussion of our theoretical approach is reserved for the Appendixes. In Sec. III we report an experimental test of our theoretical predictions by applying our AFM technique to a macroscopic model system that mimics the situation of a bacterial cell. In Sec. IV we describe the procedures applied in our experiments on bacteria. In Sec. V we report the results of our measurements performed on *Magnetospirillum gryphiswaldense* and the data are discussed in Sec. VI, while Sec. VII summarizes our conclusions.

II. THEORETICAL DESCRIPTION OF THE INDENTATION OF THE BACTERIAL ENVELOPE BY THE AFM CANTILEVER

From the mechanical point of view the bacterial envelope can be considered as a composite elastic shell. In general, the deformation is expected to be a nonlinear function of the force. In the present work we consider only small deformations of the envelope, which can then be treated within the framework of a linear elastic theory. This assumption is supported by our observations that the relationship between the depth of the indentation and the applied force is linear, but also by previous experiments [21–23]. We therefore assume that the bacterial envelope can be characterized by an elastic modulus characterizing the relationship between the deformation of the composite shell and the applied force.

In this paper we consider the experimental situation of a bacterium attached to a substrate. The probing AFM tip (having approximately the form of a rounded cone) causes an indentation on the bacterium from above [Fig. 1(a)]. The bacterial envelope represents a convex shell and its shape is determined by the turgor pressure. In principle, the stress within the deformed bacterial shell is determined by several contributions: bending, the intrinsic surface tension, and the additional stretching caused by the induced deformation. For small deformations such as produced in our AFM experiments the tangential displacements of the bacterial shell are negligible compared to the displacement perpendicular to the surface. In the following the latter is referred to as a ''normal displacement'' and we characterize it in terms of the function ψ, which gives the displacement in the direction normal to the initial (nondeformed) surface of the shell [as shown in Fig. 1(b) with its maximum absolute value denoted as δ, $\max|\psi|=\delta$] and depends on the surface coordinates (Fig. 1).

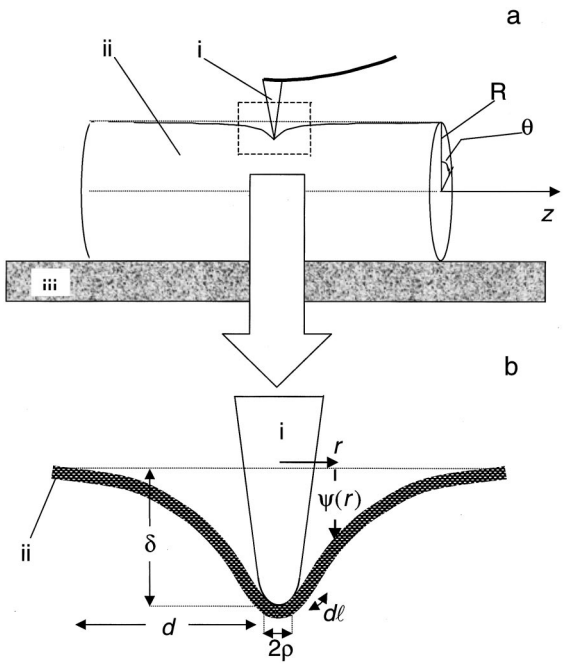

FIG. 1. Schematic view of the indentation of the bacterial wall formed by the cantilever. (i) the cantilever; (ii) the bacterial cell envelope; (iii) the substrate. (a) General view of a cylindrical fragment of the bacterium and the indention formed by the AFM cantilever. (b) We show here the vicinity of the cantilever tip, the contact domain (diameter 2ρ), the element dl of the contour ''drawn'' on the surface of the envelope in such a way that it is normal to the contact contour, the surface displacement $\psi(r)$, the indentation depth δ, and the cutoff distance d.

Considering the bacterial envelope as a thin shell, one finds that the energy of bending per unit area is proportional to the square of the local curvature (analogous to the case of biomembranes [24]). It can be expressed as $k_c(\Delta\psi)^2$, where Δ is the Laplace operator and k_c the bending elastic modulus of the shell [25] (for detailed calculations, see [26]). The cantilever applies a localized force to the bacterial surface. In this case the displacement decays to zero within the length scale d [25]. Since $\Delta\psi$ can be estimated as ψ/d^2, one finds the contribution of the bending energy per unit area F_b to be of the order of $k_c\psi^2/d^4$ [25,27]. In the same manner, the contribution of the surface tension to the free energy per unit area can be estimated as $F_t\sim\sigma(\nabla\psi)^2\sim\sigma\psi^2/d^2$, where σ is the surface tension of the envelope caused by the turgor pressure. Finally, the surface area is stretched during the deformation by the AFM tip. The stretching can be characterized by the area change $\delta dA/dA$, where dA is the element of the surface area of the bacterial envelope and δdA is its variation under the surface displacement. This ratio can be expressed as $\delta dA/dA\sim\psi/R$. The origin of this relation is discussed in detail in Appendix A. Hence, one can estimate the

TABLE I. Values and estimates of the bacterial parameters.

Specification of the parameter	Measured or estimated value of the parameter	References
Young's modulus of the envelope E	3×10^{7} Pa	[22,23]
Bacterial radius R	5×10^{-7} m	Our measurement
Thickness of the bacterial envelope h	10^{-8} m	[1,2]
Radius of the cantilever tip ρ	5×10^{-9} to 10^{-8} m	Our measurement
Turgor pressure p for gram-negative bacteria	$\sim10^{5}$ Pa	[1,2,5–9]
Length of *Magneto-spirillum gryphiswaldense* cells L	3 to 6 μm	Our measurement
Regime parameter κ	30 to 100	Our estimate
Stretching modulus of the bacterial envelop λ	$\sim10^{-1}$ Pa m	Our estimate
Cutoff distance d	$\sim10^{-7}$ m	Our estimate

contribution of the stretching energy per unit area F_{st} as $F_{st}\sim\lambda\psi^2/R^2$, where λ is the lateral modulus of compression. The total free energy of the envelope is the sum of these terms: $F=F_b+F_t+F_{st}$.

The dimensionless parameter $\kappa=F_t/F_b=\sigma d^2/k_c$ distinguishes between the bending- and the tension-dominated regimes. Assuming $\kappa\ll1$ one finds a bending-dominated regime $F_b\gg F_t$. In this regime $F\approx F_b+F_{st}$ applies. Minimization of the total energy F with respect to d yields a finite value of the cutoff distance $d^4\sim k_cR^2/\lambda$ [25]. In this case $F_b\sim F_{st}$. In contrast, $\kappa\gg1$ determines a tension-dominated regime $F_b\ll F_{st}\sim F_t$. In this regime one finds again a finite cutoff distance $d^2\sim\sigma R^2/\lambda$. One can estimate the bending modulus of a shell in terms of the Young's modulus according to $k_c\sim Eh^3$ [25], where h is the shell thickness. In the shell theory the lateral stretching modulus appears as the result of integration of the shell free energy over the shell thickness, hence $\lambda\sim Eh$ [25]. Finally, making use of the Laplace relation between surface tension and curvature, $\sigma\sim pR$, one obtains the following expression for the parameter κ:

$$\kappa\sim\frac{pR^2}{Eh^2}. \tag{1}$$

The Young's modulus of the bacterial wall has been measured for *Bacillus subtilis* and is $E\approx30$ MPa [23]. By substituting the turgor pressure ($p\sim100$ kPa) and the bacterial size ($R\sim1$ μm) measured in our experiment (Table I) one finds that the value of κ is of the order of 50. One can therefore conclude that the bacterial envelope is in the tension-dominated regime.

We thus conclude that the mechanical equilibrium of the bacterial shell is determined by its surface tension as well as its stretching and the turgor pressure. In contrast, the envelope bending plays a negligible role. Hence, the free energy describing the state of the bacterial envelope deformed by the cantilever can be expressed in the form

$$F=\oint\!\!\oint\left[\sigma+\frac{\lambda}{2}\left(\frac{\delta A}{A}\right)^2-(\mathbf{f}\cdot\mathbf{n})\psi\right]dA-p\iiint dV. \tag{2}$$

In this equation $p=p_{cyt}-p_{ext}$ is the turgor pressure, which is equal to the difference between the osmotic pressure in the cytoplasm (p_{cyt}) and in the external medium (p_{ext}). The first term of this equation accounts for the total deformation energy of the cell envelope and the integration runs over the whole bacterial surface area. The first term under the integral is the surface tension caused by the bacterial turgor pressure. The second term is the elastic energy cost associated with the lateral stretching of the bacterial envelope caused by its local displacement in the normal direction and is determined by the lateral compressibility of the envelope. The third term is the gain in potential energy due to the extrinsic force $\mathbf{f}$ per unit area exerted on the envelope. Here $\mathbf{n}$ is the outer normal to the surface. The scalar product $(\mathbf{f}\cdot\mathbf{n})$ is the normal component of the force per unit area. The volume integral on the right side accounts for the work of the turgor pressure $p=p_{cyt}-p_{ext}$ associated with the change in volume. A mathematical complication arises due to the anisotropy of the surface tension σ (which is equal to the surface energy per unit area). The component of this stress in the direction of the cylinder axis, σ_{zz}, differs from the transverse component σ_{ss}. However, the AFM technique does not allow one to measure the components separately. We therefore assume an average tensile strength $\sigma=(\sigma_{ss}+\sigma_{zz})/2$.

The general relationship between deformation of the envelope and the external force is obtained by minimizing the total free energy with respect to the deformation ψ: $\delta F/\delta\psi=0$. In order to simplify the mathematical problem we consider only bacteria with cylindrical shapes such as *Magnetospirillum gryphiswaldense*. We characterize the surface of the shell by the radius vector $\mathbf{R}=(R\cos\theta,R\sin\theta,z)$, where R is the radius of the bacterial envelope, while θ and z are the cylindrical coordinates defined in Fig. 1(a). For a force acting in the direction normal to the envelope and for small indentations of the cantilever, the main contribution to the deformation is determined by the normal displacement

$\psi=\psi(\theta,z)$. The displacements in the tangential direction are negligible. The deformed bacterial surface can be described by a new radius vector $\mathbf{R}'$ represented as

$$\mathbf{R}'=\mathbf{R}+\mathbf{n}\psi. \tag{3}$$

Note that since the displacement is directed toward the inside of the bacterium, one finds $\psi(\theta,z)\leqslant 0$. The bacterial free energy Eq. (2) together with the parametrization Eq. (3) yield the expression for the energy cost of the deformation of the bacterial envelope by the cantilever (Appendix A),

$$F=F_0+\oiint\left(\frac{\sigma}{2}(\nabla\psi)^2+\frac{\lambda-pR}{2R^2}\psi^2-(\mathbf{f}\cdot\mathbf{n})\psi\right)dA, \tag{4}$$

where F_0 is the elastic energy of the nondeformed cell envelope. By minimizing this free energy Eq. (4) in the deformed state, one obtains the Euler-Lagrange equation

$$\left\{\frac{1}{R^2}\frac{\partial^2\psi}{\partial\theta^2}+\frac{\partial^2\psi}{\partial z^2}\right\}-\frac{1}{d^2}\psi=\frac{4f}{3pR} \tag{5}$$

with

$$d^2=\frac{3pR^3}{4(\lambda-pR)}. \tag{6}$$

Here $f=-(\mathbf{f}\cdot\mathbf{n})$ is the absolute value of the normal component of the force per unit area (in other words, it represents the pressure that the cantilever tip exerts on the envelope). The minus sign reflects the fact that the force is directed toward the inside of the bacterium. The cantilever pressure $f=f(\theta,z)$ varies as a function of the surface coordinates and vanishes outside the contact domain. Note that d in Eq. (6) is a characteristic length scale. It can be interpreted as the distance from the tip of the cantilever at which the normal displacement of the membrane vanishes. This cutoff radius of the deformation can be estimated by inserting the values of the parameters R, λ, and p (summarized in Table I) in Eq. (6), yielding $d\sim 10^{-7}$ m. For $p<\lambda/R$ the free energy F has a global minimum and the cylindrical bacterial shell is stable. In the opposite case ($p\geqslant\lambda/R$) the shell is unstable and is expected either to swell or to undergo mechanical fracture. Analysis shows, however, that osmotic lysis of bacteria should occur even below the critical value of the turgor pressure $p_{cr}=\lambda/R$; moreover, it is probably related to the start of activity of the so-called lytic enzymes[8,28,29] rather than to the purely mechanical fracture.

Solving Eq. (5), which describes the deformation of the envelope by the cantilever tip (Appendix C), one finds the spring constant k_s of the envelope:

$$k_s=\frac{3\pi}{2}pR\varphi(\rho/d) \tag{7}$$

with the geometric factor $\varphi(\rho/d)=\rho K_1(\rho/d)[dK_0(\rho/d)]^{-1}$, where $K_0(\rho/d)$ and $K_1(\rho/d)$ are modified Bessel's functions and ρ is the radius of the contour of the contact of the cantilever tip with the bacterial envelope [Fig. 1(b)]. The behavior of the geometric factor $\varphi(\rho/d)$ in the interval of values ρ/d corresponding to those met in our experiments is shown in Fig. 2(b).

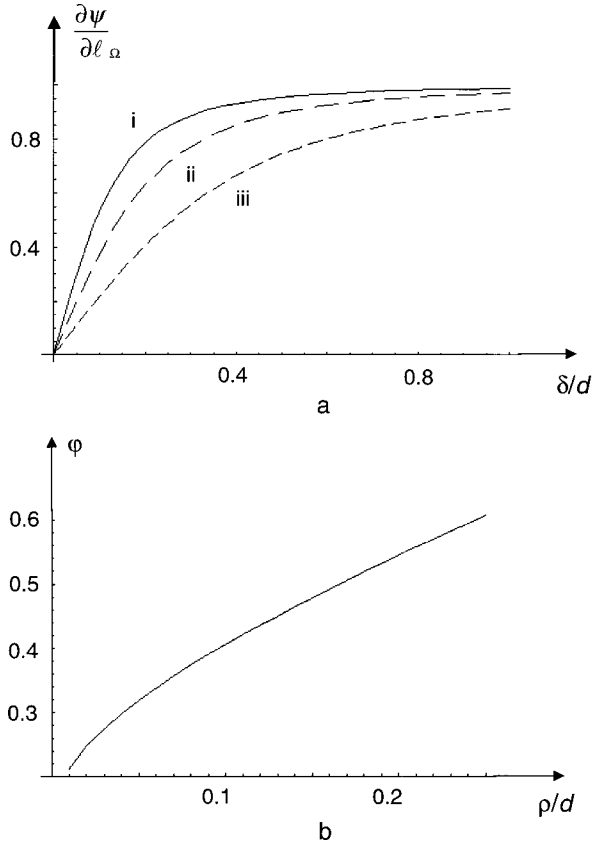

FIG. 2. (a) Variation of the displacement derivative $\partial\psi/\partial l_\Omega$ with the indentation depth δ for three ratios of ρ/d [ρ/d (i) 0.05; (ii) 0.1; (iii) 0.3]. Note that a linear law holds for small ρ/d. (b) Dependence of the geometric factor φ on the ratio ρ/d.

III. ANALOGOUS EXPERIMENT

The applicability of the present theory has been verified by a model experiment. A rubber tube with a radius $R=28$ mm and a wall thickness $h=0.4$ mm, inflated by the pressure $p=25$ kPa, was indented with a sphere with a radius of about 3 mm. The Young's modulus E of the rubber tube measured in a separate experiment was about 1.6 MPa. The Poisson's ratio $\nu\approx 0.499\,89$ [30] was used. These values yield $\lambda=Eh/(1-\nu^2)\approx 832.2$ Pa, and correspond to $\kappa>20$ in Eq. (1), ensuring that the tube is in the tension-dominated regime. We varied the indentation depth from 0 to 20 mm in steps of 1 mm and measured the corresponding force applied to the tube. A linear relationship between force and indentation was indeed observed and an effective force constant of the inflated rubber tube of $k_s\approx 0.7$ kN/m was found. To estimate the cutoff radius we measured the distance from the point where the force has been applied to that at which the displacement value decreased twofold (with respect to the indentation values of 10 and 20 mm, respectively). We found a distance of 7 mm. Making use of the solution for the displacement Eq. (C2) (Appendix C) one finds the equation $1.5K_0(3/d)=K_0(7/d)$, whose solution yields the cutoff radius $d\approx 31$ mm. The cutoff radius calculated by inserting the corresponding values in Eq. (6) is $d=52$ mm, in good agreement with the measured value. We could not measure the value of the contact contour radius ρ, which is, however, expected to be close to the radius of the indented sphere. The calculated cutoff radius value $d=52$ mm yields for the geo-

metric factor $\varphi(\rho/d)\approx 0.335$. Making use of Eq. (7) and taking into account the measured force constant of $k_s = 0.7\,\mathrm{kN/m}$, one obtains for the ''turgor'' pressure 16 kPa. This is rather close to the pressure actually applied. The reasonable agreement of the present theory with a macroscopic analogous experiment convinces us that the theoretical approach presented in this paper is suitable for calculating the turgor pressure of bacteria.

IV. MATERIALS AND METHODS

A. Treatment of cover glasses

Cover glasses (diameter 16 mm, thickness 0.1 mm) were incubated in Piranha solution (70 vol % concentrated H_2SO_4 and 30 vol % of 30% H_2O_2) for 2 h at room temperature to remove contamination. The cover glasses (usually 10 pieces in a rack) were then rinsed 10 times in about 200 ml deionized water and dried at 150 °C for 30 min.

B. Silanization of the cover glasses

Silane trimethoxysilyl-propyl-diethylenetriamine (DETA, United Chemical Technologies, Bristol, USA) was hydrolyzed at a concentration of 1 vol % in 1 m*M* acetic acid for 5 min. The clean cover glasses were incubated in the solution for 2 min and then extensively rinsed in deionized water. Then the coated cover glasses were ultrasonicated for 15 min at room temperature in deionized water in a Bandelin Sonorex RK 102 (Bandelin, Berlin, Germany). These coated and cleaned cover glasses were annealed in an oven at 150 °C for 30 min.

C. Stock suspension of bacteria

Cells of *M. gryphiswaldense* (DSM6361) strain MSR-1 [31] were used in all experiments. Bacteria were cultivated using a growth medium described elsewhere [32]. In brief, the cells were grown at 30 °C in a medium containing (per liter) 0.5 g KH_2PO_4, 1.0 g sodium acetate, 1.0 g soybean peptone (Merck, Darmstadt, Germany), 0.1 g NH_4Cl, 0.1 g $MgSO_4 \cdot 7H_2O$, and 0.1 g yeast extract. The concentration of iron in the growth medium was held at 15 μM. Before storing at −80 °C, 20% glycerol was added to the cell suspension and 60 μl aliquots were shock frozen in liquid nitrogen. Shortly before the experiment an aliquot was thawed and centrifuged at 10 000*g* for 5 min. The pellet was resuspended with 60 μl of buffer solution (5 m*M* Hepes *p*H 7 and 10 m*M* NaCl).

D. Preparation of the bacteria for imaging

15 μl of the bacterial suspension in Hepes buffer were incubated for 10 min on a DETA-coated cover glass. During the incubation another cover glass without coating was placed on top of it (''sandwich technique''). To remove the upper cover glass a droplet of Hepes buffer was placed at the edge of the ''sandwich.'' Capillary forces sucked the droplet between the cover glasses, and the upper one could then be removed horizontally. During the procedure more Hepes buffer was added in such a way that the sample was never allowed to dry and could be imaged directly with the AFM.

Scanning electron microscopy (SEM) investigations were done on the bacteria. For this purpose the remaining buffer was sucked off with a filter paper after the upper cover glass had been removed. For the control sample no upper cover glass was used during the incubation. The samples were dried at room temperature and sputtered with gold with a BAL-TEC SCD005 (BAL-TEC AG, Balzers, Liechtenstein) for 6 min in an argon environment under a pressure of 10^{-1} mbar, resulting in a thickness of the gold layer of 150–200 Å.

E. AFM imaging

Imaging and force mapping were performed with a MultiMode-SPM Nanoscope IIIa (Digital Instruments, Santa Barbara, California). A ''J'' scanner (AS-130, Digital Instruments) was used.

F. SEM imaging

SEM was carried out on a JEOL JSM-5900LV (JEOL Ltd., Akishima, Japan). The coated samples were examined with beam energies of 10 and 20 kV.

V. RESULTS

A. Immobilization of the bacteria on a surface

An important requirement for AFM investigations is that the sample can be immobilized on a surface. This can occur by means of van der Waals forces, electrostatic forces, hy-

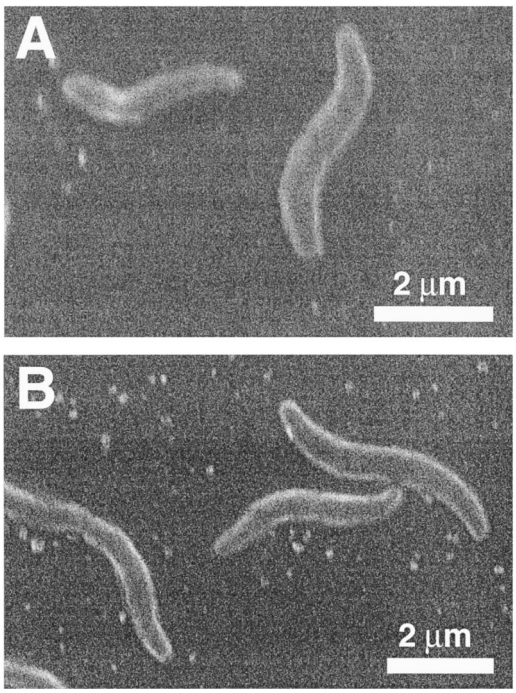

FIG. 3. SEM images of *M. gryphiswaldense*. (a) *M. gryphiswaldense* prepared by the sandwich technique used for AFM imaging (see also Sec. IV). The beam energy was 10 kV. (b) *M. gryphiswaldense* adsorbed to a cover glass without the sandwich technique. No second cover glass was used during the incubation of the bacterial suspension. The beam energy was 20 kV. The shapes of the bacteria are not influenced by the different preparation techniques.

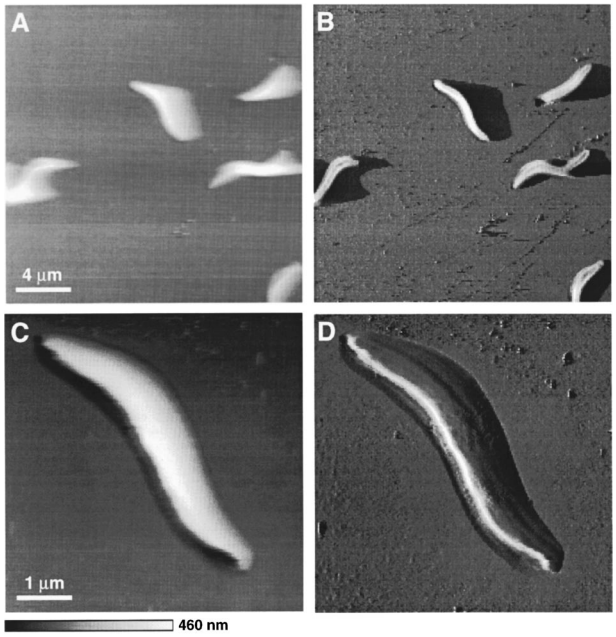

FIG. 4. Tapping mode image of *M. gryphiswaldense* cells in buffer solution. The cells were adsorbed on DETA by the sandwich technique. (a) and (c): Height signal. (b) and (d): Error signal, which reflects the small surface corrugations. (a) and (b) show an overview of a scan range of 24 μm. The membrane looks smooth.

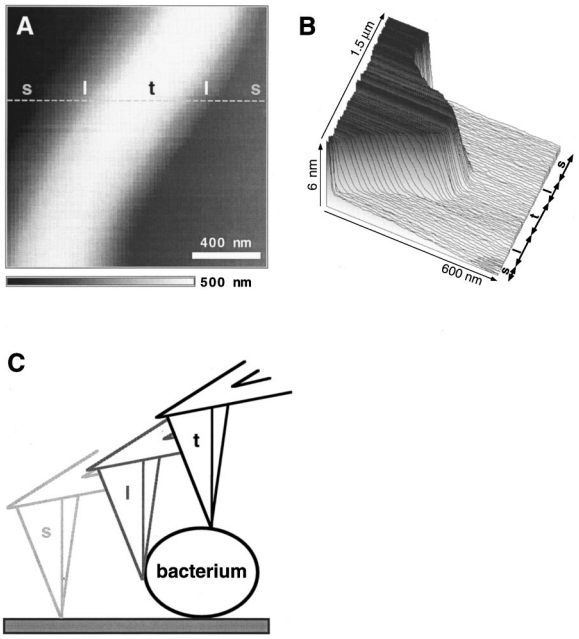

FIG. 5. Force mapping of intact bacteria. (a) Reconstructed height of the middle part of *M. gryphiswaldense*. The gray scale of the height is given below. This image has been obtained by plotting the point of contact of each force curve of the two-dimensional array of force curves. It shows the topography of the cell at minimum force. The characters *s*, *l*, and *t* indicate the substrate, the lateral contact, and the top of the bacterium, respectively. (b) Plot of force curves along dashed line in (a). Note that the force curves on the substrate (*s*) are very steep because of its low compressibility while they are shallow on the edge of the bacterium (*l*) because the tip slides laterally along the sidewall. The force curves on top of the bacterium (*t*) reflect the compressibility of the cell. These curves are the only ones taken for analysis of the turgor pressure. (c) Schematic drawing of a tip scanning over a bacterium. The letters correspond to the letters in (a) and (b).

drophobic interactions, covalent bonds, or a mixture of those forces. For the adsorption of *M. gryphiswaldense* on a solid surface we tried several procedures, like coating glass or mica surfaces with lysine, concanavalin *A*, CellTak (a mixture of cell adhesion proteins from mussels, Becton & Dickinson, purchased from Labor Schubert, München, Germany), and DETA. None of the methods resulted in a strong enough anchoring of the bacteria to the surface. Only the previously described sandwich technique, where the bacteria were enclosed between a DETA-coated cover glass and a plain cover glass, led to such a strong binding of the cells that they could be investigated by AFM. The bacteria had to be forced close to the coated surface in order to minimize the length of diffusion. The shear forces while removing the upper glass are assumed to be mainly responsible for the strong adhesion as they might press the bacteria to the surface.

SEM control measurements indicate that the shear force deposition method (''sandwich technique'') caused no alterations of either the shape or the surface of the bacteria. Figure 3 shows SEM images of *M. gryphiswaldense* prepared with the sandwich technique (a) and without (b). No surface structure is visible. No surface alterations due to the preparation technique can be seen.

By making use of the AFM the cells could be imaged in buffer solution and showed an even and random distribution on the surface. Their length was about 3 to 6 μm and their height about 500 nm. These dimensions agree well with observations in the transmission electron microscope and with the light microscope. The spiral structure is clearly visible (Fig. 4). Figures 4(a) and 4(c) show the height signal, Figs. 4(b) and 4(d) the error signal. The latter reflects the small surface corrugations [33]. The surface of the bacteria appears smooth and almost structureless. The thick layer of lipopolysaccharides and lipoproteins which is covalently attached to the peptidoglycan sheet forms a gel-like mantle and may be too soft to resolve single structures within the imaging resolution of the AFM [34].

B. Laterally resolved force mapping on the cells

For force mapping only intact bacteria were chosen exhibiting a height of at least 500 nm. Indentation data for bacteria were included in the analysis only if the original shape height of the envelope fully recovered after deformation. This means that the deformation was purely elastic, reversible, and reproducible. We are confident that under these conditions we measure the properties of intact cell envelopes.

In the force mapping mode force curves are taken while scanning laterally over the sample [35]. In Fig. 5(a) reconstructed height signals are shown, while Fig. 5(b) shows force curves along the indicated line. The letters in Fig. 5(a) along the dashed line correspond to the letters in Fig. 5(b) along the force curves and to the letters in the sketch of Fig. 5(c). On the substrate (*s*) the slope of the force curves is equal to 1, because the substrate is almost incompressible. A region (*l*) appears on the bacterium where the tip touches the cell laterally [cf. Fig. 5(c)] and the tip is expected to slide sideways over the edge of the bacterium. As the contact area

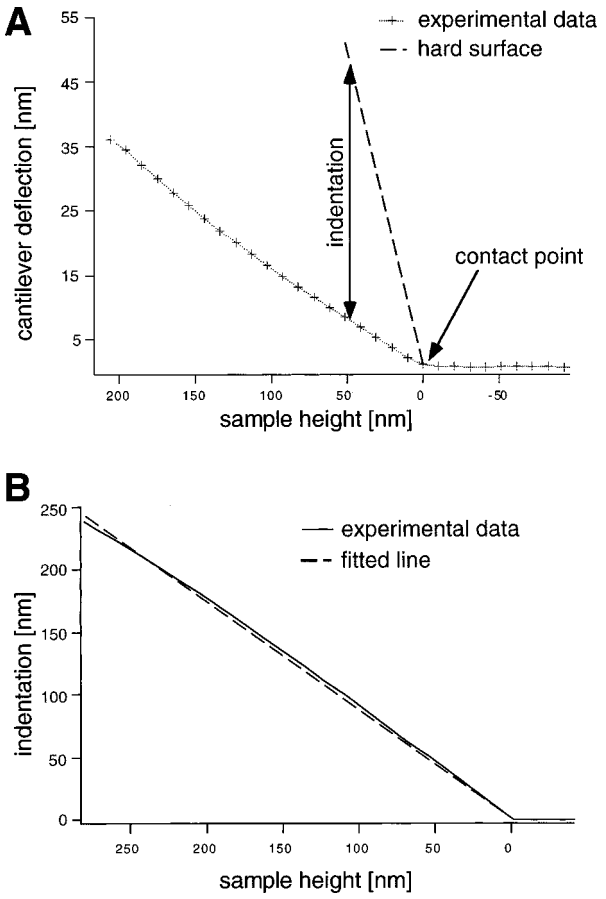

FIG. 6. Relationship between cantilever deflection and indentation of the sample. (a) Comparison of force curve on top of bacterium (experimental data) and theoretical force curve on a hard surface. The difference between the two force curves yields the curve representing the indentation of the tip in the sample in (b). (b) Indentation of the tip in the bacterium versus sample height. With the indentation and the given spring constant of the cantilever we calculate the spring constant k_s of the bacterium.

of the tip is not known in this case, those data cannot be evaluated and are not included in our analysis. Only force curves taken on top of the cell (region *t*) [Figs. 5(a)–5(c)] were considered further since the contact area of the tip is well defined in this region.

In Fig. 6 the relationship between cantilever deflection and indentation of the cell envelope is shown. The indentation can be calculated by subtracting the cantilever deflection on the bacterium from the cantilever deflection on the substrate [Figs. 6(a) and 6(b)] [34]. With the known indentation and the spring constant of the cantilever the effective spring constant of the bacterial cell envelope can be calculated, as will be outlined below (Table II).

C. Turgor pressure of *M. gryphiswaldense*

The outer membrane of the gram-negative bacterium *M. gryphiswaldense* serves several functions. It acts as a molecular sieve, as a carrier of antigens and receptors, and most important it counterbalances the internal turgor pressure. In this function it is important to know that the outer membrane is covalently bound to the peptidoglycan sheet and together with this sheet and the inner membrane forms the cell envelope. The turgor pressure of *M. gryphiswaldense* has not been measured so far to our knowledge. However, based on the literature data for gram-negative bacteria one can expect it to be in the range from 10^4 to 10^5 Pa.

D. Spring constant of the bacterial cell envelope

The force curve presented in Fig. 7(b) shows a linear response of the bacterium when loading it with the AFM tip. The model developed above (Sec. II) predicts a linear relationship between force and indentation, which has also been observed in our macroscopic model experiment. This suggests that the observed linear force-indentation relation is due to the turgor pressure.

Since the elastic response of the bacterial cell envelope is linear, we can define an effective force constant that characterizes the rigidity of the whole bacterium. The experimental setup may be represented by two linear springs in series, one being the AFM's cantilever and the other the cell envelope exhibiting an effective force constant. We can then calculate the effective force constant k_s of the cell envelope from the observed slope s of the force curve and the known force constant k_c of the cantilever, according to

$$k_s = \frac{k_c s}{1-s}. \tag{8}$$

The first row of Table III shows the effective force constant as determined from the force map of Fig. 7.

With the radius of $\rho = 5\times10^{-9}$ m of the cantilever used and the estimated value of the cutoff radius ($d \sim 10^{-7}$ m), one finds $\rho/d = 0.05$. In the AFM experiments one can generally expect to find the values ρ/d in the interval from 0.01 to 0.1. The corresponding value of the geometric factor

TABLE II. The effective force constant as determined from the force maps and the turgor pressure of different bacteria studied in this work.

	Bacterium						
	1	2	3	4	5	6	7
k_c (N/m) ($\pm$0.01)	0.24	0.23	0.21	0.25	0.23	0.32	0.21
s	0.15	0.14	0.18	0.19	0.24	0.14	0.18
	$\pm$0.03	$\pm$0.02	$\pm$0.02	$\pm$0.02	$\pm$0.03	$\pm$0.02	$\pm$0.02
k_s (N/m) ($\pm$0.01)	0.04	0.04	0.05	0.06	0.07	0.04	0.05
p (MPa) $\varphi = 0.2$	0.085	0.085	0.106	0.127	0.149	0.085	0.106

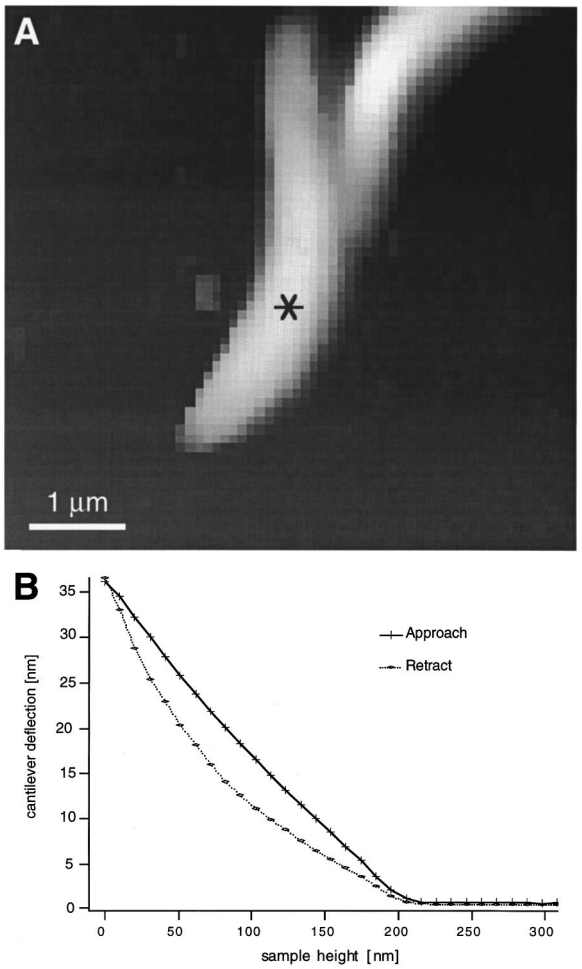

FIG. 7. Force mapping on intact bacteria. (a) Reconstructed height signal of intact bacteria. (b) Force versus distance curve during approach to bacterium at point marked by the asterisk. Note that the linear relationship agrees with the theoretical approach (Sec. II), predicting a linear force-indentation relation for a cylindrical shell, and with the model experiment described in Sec. III.

$\varphi(\rho/d)$ varies from 0.22 to 0.4 [Fig. 2(b)]. Making use of the expression Eq. (7), the measured values k_s summarized in Table II, and assuming a value of $\varphi=0.2$, one obtains turgor pressure values in the range of $p=85$ to 150 kPa (Table II).

VI. DISCUSSION

We present here a theory enabling the application of the AFM technique to measure bacterial turgor pressure. The theoretical approach presented here is based on two inequalities. The first of them, $\kappa \gg 1$, distinguishes between the bending- and tension-dominated regimes. The estimate $\kappa \sim 50-100$ follows from the bacterial parameters listed in Table I and reliably shows that the bacterial envelope is in the tension-dominated regime due to the high turgor pressure. This enables us to reduce the free energy to a relatively simple form, Eq. (2). The equation of equilibrium (5) following from Eq. (2) is still rather complicated and cannot be solved in a general case. However, if the inequality $d/R \ll 1$ is valid the envelope curvature and the boundary conditions at the substrate play a negligible role. In this case one can use the quasiflat approximation and obtain a simple analytical solution describing the envelope bending by the AFM tip (Appendix C). Our estimate yields $d/R \approx 0.2$. Thus the validity of this inequality is not as reliable as that of the first one. However, if the second inequality break down, the quasiflat approximation still reasonably describes the deformation of the envelope. This is proved by an analogous macroscopic experiment (Sec. III), in which we measured (by a setup analogous to the AFM) a pressure that was rather close to the actual value despite the value of the ratio $d/R \approx 1.86$. This weak dependence of the force on the ratio d/R stems from the fact that in the tension-dominated regime the force exerted on the AFM tip is largely determined by the envelope shape in the close vicinity of the contour of its contact with the tip.

The above approach makes it possible to find the value of the turgor pressure by AFM measurements. We can determine the absolute value of the turgor pressure within a factor of about 2, since it depends on a ratio ρ/d that cannot be measured. However, the increase of the geometric factor φ with the ratio ρ/d is rather slow since an increase of ρ/d by an order of magnitude (from 0.01 to 0.1) results in an increase of φ by only a factor of 2 [Fig. 2(b)].

A single measurement of the elasticity at one point on top of a bacterium takes less than a second (typically only 50–100 ms). If the external osmotic pressure could be changed abruptly without disturbing the AFM (e.g., by rapid exchange of the buffer) rapid changes of the cellular stiffness could be determined by AFM. This offers the possibility of monitoring relative changes in the bacterial turgor pressure, since according to Eq. (7) a change of the turgor pressure from a value p_1 to p_2 corresponds to a change of the effective stiffness of the envelope, $k_{s2}/k_{s1}=p_2/p_1$.

Application of the AFM requires attachment of the bacterium to a substrate. This may cause plasmolysis and influence the turgor pressure [14]. Plasmolysis may also be caused by the measurement itself, due to damage of the envelope by the AFM tip. We observed this kind of phenomenon in some of our measurements.

In addition to the measurements under constant osmotic conditions, we tried the effect of changes in external osmolarity on the bacterial turgor pressure by addition of sucrose to the solution. We did not observe any changes in the rigidity of the bacteria (Table III). This insensitivity to changes of the osmolarity is probably due to the fact that the measurements were performed within several tens of minutes after the bacteria were placed into the medium with the increased osmolarity, so that they could have adapted to the change of the external medium before the measurement was started.

VII. CONCLUSIONS

We have presented a theory for AFM measurements of bacterial turgor pressure. It predicts that the spring constant of the bacteria measured by AFM is proportional to the turgor pressure. We have shown that the AFM technique enables measurements of bacterial turgor pressures within a factor of 2 (depending on the ratio of the AFM tip radius to the cutoff radius). We made experiments on *Magnetospirillum gryphiswaldense* and determined the turgor pressure to be in the range of 85 to 150 kPa.

TABLE III. Effective force constant of the bacteria determined from the force maps corresponding to Fig. 7.

Medium sucrose (mM)	Slope	Measurements	Effective force constant (N m^{-1})	Standard deviation
0	0.18	654	42×10^{-3}	4.4×10^{-3}
50	0.18	550	42×10^{-3}	4.4×10^{-3}
100	0.18	448	42×10^{-3}	4.4×10^{-3}
150	0.18	493	42×10^{-3}	4.4×10^{-3}

ACKNOWLEDGMENTS

This work was supported by the Deutsche Forschungsgemeinschaft (M.A., M.R., M.F., E.S). One of the authors, A.B., was partially supported by the Alexander von Humboldt Foundation and by the Deutsche Forschungsgemeinschaft, Grant No. SA 246/28-1.

APPENDIX A: THE FREE ENERGY OF DEFORMATION OF THE BACTERIAL ENVELOPE

The parametrization (3) describes the variation of the radius vector of the surface during the indentation of the AFM tip. The indentation leads to a change in the area of the envelope and of the volume of the cell. Following Zhong-Can and Helfrich [26] these variations can be expressed as functions of the displacement ψ as

$$\delta A=\oiint[-2H\psi+\tfrac{1}{2}(\nabla\psi)^2+K\psi^2]dA,$$

$$\delta V=\oiint(\psi-H\psi^2)dA. \tag{A1}$$

In this equation $H=(R_1^{-1}+R_2^{-1})/2$ is the mean curvature and $K=R_1^{-1}R_2^{-1}$ is the Gaussian curvature of the undeformed surface, and R_1 and R_2 are the principal surface curvature radii. For the case of a cylindrical surface ($R_1=R$, $R_2=\infty$) we have $H=-(2R)^{-1}$ and $K=0$. Note that the second term in the expression for δA is expressed in terms of the covariant derivatives $(\nabla\psi)^2\equiv g^{ij}\nabla_i\psi\nabla_j\psi$, where $\nabla_i\equiv\partial/\partial\xi^i$ with the cylindrical surface coordinates $\xi^1=\theta$ and $\xi^2=z$. Here g^{ij} is the contravariant metric tensor of the surface. For the case of a cylinder the components of the metric tensor take the form

$$g_{11}=R^2,\quad g^{11}=R^{-2},\quad g_{22}=g^{22}=1,\quad g_{12}=g^{12}=0 \tag{A2}$$

[36,26]. The item $\sim(\nabla\psi)^2$ in the expression (A1) corresponds to the well-known Monge term that appears in the theory of strong bending of initially flat plates [25]. In contrast, the first term $(-2H\psi)$ in the expression for δA [Eq. (A1)] has a purely geometrical nature and vanishes for the initially flat surface at $H\to0$ (i.e., $R\to\infty$). However, it plays the primary role in the present case of a strongly curved surface. Turning from the integral expression (A1) for δA to the differential relation for the area elements one finds for the cylindrical surface

$$\delta\,dA=[-2H\psi+\tfrac{1}{2}(\nabla\psi)^2]dA\approx-2H\psi\,dA. \tag{A3}$$

This expression yields the estimate for $\delta\,dA/dA$ used in Sec. II.

Substituting Eq. (A3) into the free energy Eq. (2) and performing the variation of the cylinder length $L'=L+\delta L$ makes it possible to express the free energy variation under indentation as a functional of the envelope displacement $\delta F=\delta F\{\psi\}$:

$$\delta F=\pi R\,\delta L(2\sigma_{zz}-pR)+\oiint\left[\left(\frac{\sigma_{ss}}{R}-p\right)\psi+\left(\frac{\sigma_{ss}}{2}(\nabla\psi)^2+\frac{\lambda-pR}{2R^2}\psi^2-(\mathbf{f}\cdot\mathbf{n})\psi\right)\right]dA. \tag{A4}$$

The initial cylindrical shell form must correspond to an equilibrium state. This condition is fulfilled if the terms linear in δL and ψ become zero [26]. Since the normal force $(\mathbf{f}\cdot\mathbf{n})$ gives rise to the displacement ψ, the term $(\mathbf{f}\cdot\mathbf{n})\psi$ is of the order of magnitude of ψ^2 and should be included in the quadratic part of the free energy. The terms of the free energy linear in δL and ψ vanish if

$$\sigma_{zz}=pR/2,\quad \sigma_{ss}=pR. \tag{A5}$$

These conditions yield the Laplace law for a closed cylindrical surface. Thus one finds the average tension $\sigma=3pR/4$. Taking Eq. (A5) into account one obtains the free energy of the deformation of the bacterial envelope, Eq. (4).

APPENDIX B: THE FORCE BALANCING THE CANTILEVER

In the following we calculate the force of the bacterial shell balancing the force exerted by the AFM tip. For simplicity we assume that it can be considered as a rigid conical body with a rounded tip. Therefore the contact line between the tip and the bacterial wall, Ω, is a circle of a radius ρ. In practice the AFM tip has an irregular, nearly pyramidal shape, whose details usually cannot be defined. However, in the tension-dominated regime fine details of the shape of the cantilever tip do not play an important role. We assume that the contact contour Ω has a radius ρ that is approximately equal to the radius of the rounded part of the AFM tip.

With the above simplification we can now calculate the total force f_t exerted by the cell envelope on the cantilever, which is obtained by integrating the pressure of the cantilever f over the area of the domain of contact between the cantilever tip and the membrane:

$$f_t = \iint_{\Sigma} f(\theta,z)\,dA. \tag{B1}$$

To achieve this we integrate Eq. (5) over the area of the contact domain Σ and transform the integration over the area of the two terms in its left-hand side into an integration over the contour Ω of the contact line. For this purpose we make use of the version of the well known Gaussian theorem valid for surface vector fields. It relates an integral of the divergence $\mathrm{div}\,\mathbf{B} \equiv \nabla_i B^i$ of any surface vector field $\mathbf{B}$ over a surface domain Σ to a contour integral as $\int\int_{\Sigma} \nabla_i B^i dA = \oint_{\Omega} B^i m_i ds$, where m_i is a component of the unit vector $\mathbf{m} = \mathbf{m}(s)$ tangential to the surface and normal to the contour Ω at its given point (specified by s) and ds is the element of the contour arc. For our purpose it is helpful to realize that the operator in the left-hand part of Eq. (5) is the Beltrami-Laplace operator on the surface:

$$\Delta_B \psi = g^{ij}\nabla_i \nabla_j \psi = \frac{1}{R^2}\frac{\partial^2 \psi}{\partial \theta^2} + \frac{\partial^2 \psi}{\partial z^2}. \tag{B2}$$

With $B^i = g^{ij}\nabla_j \psi$ one finds $\Delta_B \psi \equiv \nabla_i B^i$. Application of the surface Gauss theorem to the first term of Eq. (5) yields $\int\int_{\Sigma} \Delta_B \psi\, dA = \oint_{\Omega} g^{ij} m_i \nabla_j \psi\, ds \equiv \oint_{\Omega} (\partial\psi/\partial l) ds$, whence

$$\int \int_{\Sigma} \Delta_B \psi\, dA = 2\pi\rho \left(\frac{\partial \psi}{\partial l}\right)_{\Omega}, \tag{B3}$$

where dl is the element of the arc of an additional contour drawn on the surface in such a way that it is normal to the contact contour Ω. In Eq. (B3) the derivative $\partial\psi/\partial l$ is calculated on the contour Ω.

The integral of the second term in the left-hand part of Eq. (5), $-d^{-2}\int\int_{\Sigma} \psi\, dA$, is equal to the volume between the cylinder and the indented membrane divided by d^2. It can thus be approximated as

$$-\frac{1}{d^2}\int \int_{\Sigma} \psi\, dA \approx \frac{\pi \rho^2 \delta}{3d^2}, \tag{B4}$$

where we introduce the indentation depth δ as $\delta \approx |\psi(\rho)|$. We finally obtain the following equation for the equilibrium of the total force f_t exerted by the AFM tip and the reaction force of the elastic cell envelope:

$$\frac{3}{2}\pi p R \rho \left(\frac{\partial \psi}{\partial l}\right)_{\Omega} + \frac{1}{4}\pi p R \left(\frac{\rho}{d}\right)^2 \delta = f_t. \tag{B5}$$

Therefore, the mechanical reaction of the bacteria can be interpreted in terms of an equivalent mechanical circuit consisting of two springs in series. One of them with the spring constant k_1 corresponds to the first term in the left-hand part of Eq. (B5) which stems from the contribution of the turgor pressure to the bacterial rigidity. The other with the spring constant k_2 related to the second term originates from the lateral elasticity of the bacterial envelope. We can now further simplify Eq. (B5) by estimating the second term in this equation. Since δ is the depth of indentation the expression for k_2 takes the form

$$k_2 = \frac{3}{4}\pi p R \left(\frac{\rho}{d}\right)^2. \tag{B6}$$

As noted above d is of the order of 10^{-7} m. The radius ρ of the contact contour Ω is assumed to be equal to the diameter of the AFM tip used in our experiments: $\rho \sim 5\times 10^{-9}$ to 10^{-8} m. With the values of p and R given in Table I we obtain for the spring constant $k_2 \sim 10^{-4} - 10^{-3}$ N/m. This value is two to one orders of magnitude smaller than the value we have measured experimentally. We can therefore conclude that the main contribution to the reaction force of the bacterial envelope is determined by the first term in Eq. (B5). This simplifies the equation for the force to

$$f_1 = \frac{3\pi}{2} p R \rho \left(\frac{\partial \psi}{\partial l}\right)_{\Omega}. \tag{B7}$$

APPENDIX C: BENDING OF THE BACTERIAL ENVELOPE

Outside the contact contour Ω the external force of the AFM tip is equal to zero. Therefore, Eq. (5) assumes the following form in this region:

$$\Delta_B \psi - \frac{1}{d^2}\psi = 0. \tag{C1}$$

One has to fix two boundary conditions. The first concerns the contour Ω of the contact of the tip. Since in our experiments $\delta \gg \rho$, the boundary condition reads as $\psi(\rho) = -\delta$.

The second boundary condition concerns the position of the surface of the bacterium (e.g., with respect to a substrate). One should know precisely the envelope-substrate contact contour and the shape of the envelope in its close vicinity. Since both the contour and the shape are unknown, such a solution cannot be obtained in a general case. However, if $d/R \ll 1$ the envelope curvature and the boundary conditions at the substrate play a negligible role. According to the above estimates the cutoff radius $d \sim 10^{-7}$ m is smaller than the bacterial radius R and much smaller than its length $L \sim 10^{-5}$ m (Table I). Therefore, the effect of the shell curvature appears only slightly in the local (on the scale $\sim d$) behavior of the bacterial surface and can be neglected. The minimal distance between the indentation domain and the contact contour (measured along the cylinder surface) is larger than d. Therefore, the effect of the conditions at the contact contour is also small. In this case one can adopt the following approximation [27] (referred to as ''the quasiflat approximation'') which enables one to obtain a simple analytical solution describing the envelope bending by the AFM tip. The inequality $d/R \ll 1$ makes it possible to consider the bending of the envelope locally as that of a flat elastic plate, rather than of the cylindrical shell. Thus, the shell surface can be approximately considered as an infinite plane and the Beltrami-Laplace operator $\Delta_B \psi$ on the cylindrical shell is approximated by the Laplace operator on a plane (x, z): $\Delta_B \psi \approx \Delta \psi = \partial^2 \psi/\partial x^2 + \partial^2 \psi/\partial z^2$, z being the same as the cylinder coordinate, while $dx = R\, d\theta$. We further assume that the deflection vanishes at infinity: $\psi(\infty) = 0$. Within the

quasiflat approximation this yields the second boundary condition fixing the position of the envelope with respect to the substrate.

Equation (C1) with the above boundary conditions has the following solution:

$$\psi = -\delta \frac{K_0(r/d)}{K_0(\rho/d)}, \tag{C2}$$

where $K_0(x)$ is the modified Bessel's function and r is the in-plane radius vector $r=(x^2+z^2)^{1/2}$ [cf. Fig. 1(b)]. The slope of the envelope at the contact contour Ω can be expressed as

$$\left(\frac{\partial \psi}{\partial l}\right)_{\Omega} = \left[1 + \frac{d^2}{\delta^2}\left(\frac{K_0(\rho/d)}{K_1(\rho/d)}\right)^2\right]^{-1/2}. \tag{C3}$$

The variation of $\partial\psi/\partial l_{\Omega}$ with the ratio δ/d for different values of ρ/d is shown in Fig. 2(a). One can see that at small values of ρ/d the slope is linear and one can write

$$\left(\frac{\partial \psi}{\partial l}\right)_{\Omega} \approx \frac{K_1(\rho/d)}{dK_0(\rho/d)}\,\delta. \tag{C4}$$

Substitution of this relation into the expression for the force Eq. (B7) yields Eq. (7) for the bacterial spring constant k_s.

[1] D. Voet and J. G. Voet, *Biochemistry* (Wiley, New York, 1995).
[2] J. Darnell, H. Lodish, and D. Baltimore, *Molecular Cell Biology* (Scientific American, New York, 1986).
[3] R. J. Doyle and R. E. Marquis, Trends Microbiol. **2**, 57 (1994).
[4] A. M. Whatmore and R. H. Reed, J. Gen. Microbiol. **136**, 2521 (1990).
[5] A. E. Walsby, P. K. Hayes, and R. Boje, Eur. J. Phycol. **30**, 87 (1995).
[6] J. Overmann, S. Lehmann, and N. Pfennig, Arch. Microbiol. **157**, 29 (1991).
[7] T. J. Beveridge, Can. J. Microbiol. **34**, 363 (1988).
[8] A. L. Koch, Adv. Microb. Physiol. **24**, 301 (1983).
[9] A. L. Koch and M. F. S. Pinette, J. Bacteriol. **169**, 3654 (1987).
[10] T. Erdos, G. S. Butler-Browne, and L. Rapoport, Biochimie **73**, 1219 (1991).
[11] M. O. Walderhaug *et al.*, J. Bacteriol. **174**, 2152 (1992).
[12] L. N. Csonka, Microbiol. Rev. **53**, 121 (1989).
[13] P. Mitchell, in *Biological Structure and Function*, edited by T. W. Goodwin and O. Lundberg (Academic, New York, 1961), Vol. 2, p. 581.
[14] A. L. Koch, Crit. Rev. Microbiol. **24**, 23 (1998).
[15] K. Visscher, G. J. Brakenhoff, and J. J. Krol, Cytometry **14**, 105 (1993).
[16] A. A. Garcia, W. C. Pettigrew, and J. Graham, Scanning Microsc. **7**, 577 (1993).
[17] A. Umeda, M. Saito, and K. Amako, Microbiol. Immunol. **42**, 159 (1998).
[18] P. C. Braga and D. Ricci, Antimicrob. Agents Chemother. **42**, 18 (1998).
[19] A. Razatos *et al.*, J. Biomater. Sci., Polym. Ed. **9**, 1361 (1998).
[20] W. Xu *et al.*, Scanning Microsc. **8**, 499 (1994).
[21] W. Xu *et al.*, J. Bacteriol. **178**, 3106 (1996).
[22] J. J. Thwaites and N. H. Mendelson, Int. J. Biol. Macromol. **11**, 201 (1989).
[23] J. J. Thwaites and U. C. Surana, J. Bacteriol. **173**, 197 (1991).
[24] W. Helfrich, Z. Naturforsch. C **28**, 693 (1973).
[25] L. D. Landau and E. M. Lifshitz, *Theory of Elasticity* (Pergamon, London, 1959).
[26] Ou-Yang Zhong-Can and W. Helfrich, Phys. Rev. A **39**, 5280 (1989).
[27] A. A. Boulbitch, Phys. Rev. E **57**, 2123 (1998).
[28] A. L. Koch, Microbiol. Rev. **52**, 337 (1988).
[29] J. Ruiz-Herrera *et al.*, Curr. Microbiol. **37**, 365 (1998).
[30] J. Brandrup and E. H. Immergut, *Polymer Handbook* (Wiley, New York, 1989).
[31] D. Schüler and E. Bäuerlein, Arch. Microbiol. **166**, 301 (1996).
[32] K. H. Schleifer *et al.*, Syst. Appl. Microbiol. **14**, 379 (1991).
[33] C. A. J. Putman *et al.*, Proc. SPIE **1639**, 198 (1992).
[34] M. Radmacher, M. Fritz, and P. K. Hansma, Biophys. J. **69**, 264 (1995).
[35] M. Radmacher *et al.*, Langmuir **10**, 3809 (1994).
[36] E. Kreyszig, *Differential Geometry* (Dover, New York, 1991).